Effect of Crystallization Temperature on Crystal Modifications and Crystallization Kinetics of Poly(L-lactide)

Pengju Pan, Bo Zhu, Weihua Kai, Tungalag Dong, Yoshio Inoue

Department of Biomolecular Engineering, Tokyo Institute of Technology, 4259-B-55 Nagatsuta, Midori-ku, Yokohama 226-8501, Japan

Received 29 April 2007; accepted 20 July 2007
DOI 10.1002/app.27102
Published online 11 September 2007 in Wiley InterScience (www.interscience.wiley.com).

ABSTRACT: The crystalline structure of poly(L-lactide) (PLLA) have been found to quite depend on the crystallization temperatures (T_cs), especially in the range of 100−120°C, which is usually used as the crystallization temperature for the industrial process of PLLA. The analysis of wide-angle X-ray diffraction and Fourier transformed infrared spectroscopy revealed that 110°C is a critical temperature for PLLA crystallization. At $T_c < 110$°C and $T_c \geq 110$°C, the α′ and α crystals were mainly produced, respectively. Besides, the structural feature of the α′-form was illustrated, and it was found that the α′-form has the larger unit cell dimension than that of the α-form. Moreover, the crystallization kinetics of the α′ and α crystals are different, resulting in the discontinuousness of the curves of spherulite radius growth rate (G) versus T_c and the half time in the melt-crystallization ($t_{1/2}$) versus T_c investigated by Polarized optical microscope and Differential scanning calorimetry, respectively. © 2007 Wiley Periodicals, Inc. J Appl Polym Sci 107: 54–62, 2008

Key words: poly (L-lactide); crystallization temperature; crystal modification; crystallization kinetics

INTRODUCTION

Poly (L-lactide) (PLLA), as one of promising thermoplastics among the family of environmentally friendly biodegradable polymers, has attracted increasing attention in recent years.[1] PLLA has been used as a biocompatible polymer for applications in implant materials, surgical suture, and controlled drug delivery systems.[2,3] Moreover, owing to its good mechanical properties and versatile fabrication processes, PLLA also has tremendous potential in traditional applications where common thermoplastics are employed.[4,5]

Depending on the crystallization conditions, PLLA can crystallize in three different modifications (α, β, and γ form).[6–15] The most common crystal modification, α form, is believed to be produced from the melt, cold and solution crystallization under normal conditions.[6,7] It has been reported that the chain conformation of the α form is in a ''pure'' left-handed 10_3 helix which packs into an orthorhombic unit cell.[6,8] The β form was produced by stretching the α form at very high drawing ratio and high temperature.[7,10–13] The γ form, produced through epitaxial crystallization was recently described by Cartier et al.[15] The crystallization behavior of PLLA has been already investigated extensively by many research groups,[16–28] and it has been found that the crystallization behavior of PLLA is very interesting and peculiar. The peculiar behavior is that the crystallization kinetics are discontinuous in the temperature range of 100−120°C, that is, the curve of the half time in the melt crystallization ($t_{1/2}$) versus crystallization temperature (T_c) is discontinuous and the profile of spherulite radius growth rate (G) versus T_c shows two peaks.[18,25,28] At present, there are two main proposals to explain such peculiar behavior, that is, nonpolymorphism and polymorphism interpretations. Abe et al.,[18] and Di Lorenzo[25] prefer the former one, and they proposed that the discontinuity of PLLA crystallization kinetics are correlated to regime transition in this temperature range. On the contrary, Ohtani et al.,[20] Zhang et al.,[27] and Yasuniwa et al.[28] insisted that the latter one was more reasonable. They all suggested that the normal α crystal is produced in the isothermal crystallization of PLLA at high T_c. However, Ohtani et al.[20] and Yasuniwa et al.[28] suggested that the β crystal is produced at low T_c, whereas, Zhang et al.[27] insisted that another new crystal form, α′ form, is likely to be developed at this condition.

The mechanical and thermal properties of a semicrystalline polymer strongly depend on the morphology and crystal structure.[29–38] It is well known that T_c is a key factor for the crystallization process of

Correspondence to: Y. Inoue (inoue.y.af@m.titech.ac.jp).

©2007 Wiley Periodicals, Inc.
WILEY InterScience® DISCOVER SOMETHING GREAT

polymer. Moreover, in the industrial process, PLLA usually crystallize at 100−120°C owing to the high crystallization rate in this temperature region. In addition, the research of polymorphism in the biodegradable polymer with polymorphic crystals also allows us to reveal the relationship between the structure, morphology, and biodegradability. The different crystal modifications of one polymer, even though they share the common chemical structure, may have different biodegradabilities. This is not only because of difference in the size of crystal and the degree of crystallinity but also possibly to that in the spatial orientation and packing of polymer chains in the polymorphic crystal lattice.[30,39] Therefore, to control the polymorphism for optimizing the properties and production process, it is quite important to study T_c-dependent crystallization behavior of PLLA, especially at the region of 100−120°C.

The change of T_c-induced crystalline order or perfection affects the crystalline morphology to some extent; however, in this case the crystalline morphology usually change gradually with the variation of T_c. Nevertheless, in the T_c-induced polymorphic crystallization of polymer, generally, there is a critical T_c or an exact temperature region for the transition of the different crystal modifications.[40–42] Therefore, it is considered that a detailed probe into the effect of T_c on the crystalline structure with the aid of WAXD and FTIR is of fundamental importance. It is thought that according to this investigation it is possible to found what is actually responsible for these peculiarities of PLLA crystallization. Furthermore, if these peculiarities are resulted by polymorphism, the critical T_c or temperature region can be obtained, and also the structural features of these crystal forms developed at different T_cs is able to be elucidated. For these purposes, in this study the effect of T_c on the crystalline structure of PLLA were investigated, especially in the range of 100−120°C, which has been suspected to be the critical range to produce the different crystals, within an interval of 5°C.

EXPERIMENTAL

Material

The PLLA sample (M_n = 118 kg/mol, M_w = 177 kg/mol, M_w/M_n = 1.49) was kindly supplied by Unitika. (Kyoto, Japan). Before use, the sample was purified by precipitating into ethanol from chloroform solution, and then it was dried in vacuum oven at 40°C for 1 week.

Wide-angle X-ray diffraction

The Wide-angle X-ray diffraction (WAXD) analysis for the PLLA samples prepared by isothermally melt and cold crystallization at different T_cs was carried out on a Rigaku RU-200 (Rigaku, Tokyo, Japan), working at 40 kV and 200 mA, with Ni-filtered CuKa radiation (λ = 0.15418 nm). Scans were made between Bragg angles of 5°–50° at a scanning rate of 1°/min.

FTIR spectroscopy

The transmission FTIR measurements were performed on an AIM-8800 automatic infrared microscope (Shimadzu, Kyoto, Japan). The PLLA sample was placed between 2 pieces of BaF_2 slides, and then it was melted at 200°C for 2 min before quenched to the desired T_c for the crystallization. All the crystallized samples were cooled to 23°C before the measurement. The amorphous samples were obtained by rapidly quenching the samples in liquid nitrogen after melted at 200°C for 2 min. All the IR spectra were accumulated with 16 scans and a resolution of 2 cm^{-1}.

Polarized optical microscopy

Polarized optical microscopy (POM) observation was performed on an Olympus BX90 polarizing optical microscopy (Olympus, Tokyo, Japan) equipped with a digital camera. The PLLA sample (ca. 0.2 mg) was placed between a microscope glass slide and a cover slip, and the temperature was controlled by a Mettler FP82HT hot stage. The PLLA sample was at first heated to 200°C and held for 2 min at this temperature. The sample was pressed and spread into a thin film before quenched to the desired T_c. The sizes of growing spherulites were monitored by taking microphotographs during appropriate time intervals before the spherulites impinged. Plotting the spherulite radius against the growth time, a straight line was obtained, and the slope was considered as its average radial growth rate.

Differential scanning calorimetry

The nonisothermal and isothermal crystallization behavior of PLLA was measured by a Pyris Diamond differential scanning calorimetry (DSC) instrument (Perkin-Elmer Japan, Tokyo, Japan). The scales of temperature and the heat flow at different heating rates were calibrated using an indium standard with nitrogen purging. PLLA sample (ca. 7 mg) was weighted and sealed in an aluminum pan. In the isothermal melt-crystallization, the melted samples were cooled at a rate of 100°C/min to the desired T_c after melted at 200°C for 2 min and allowed to crystallize at T_c. The cooling rate, 100°C/min, is fast enough to prevent the crystallization of PLLA, which has been confirmed by FTIR. The FTIR measurement

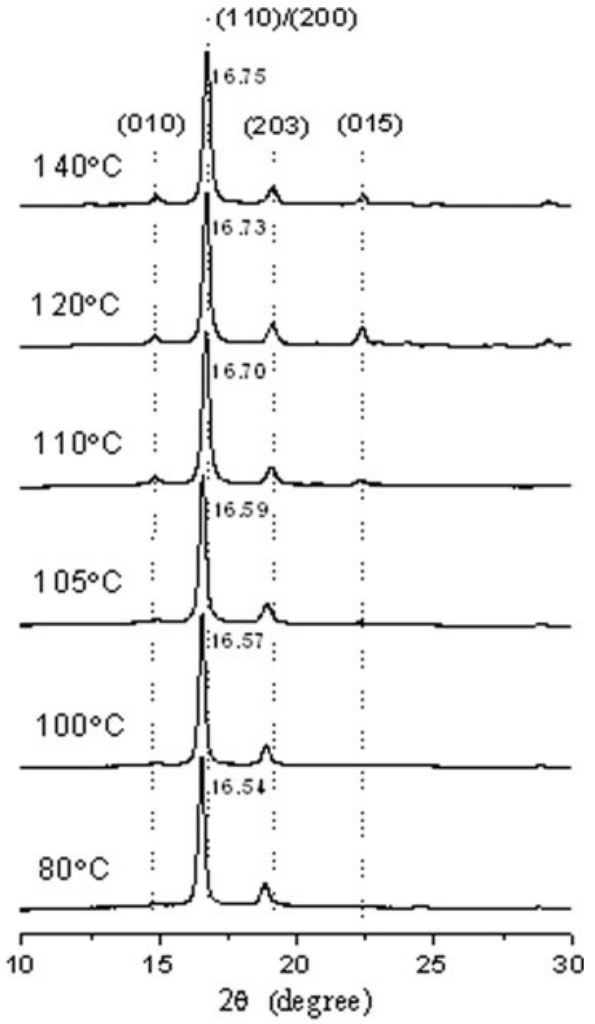

Figure 1 WAXD patterns of PLLA isothermally melt-crystallized at T_c = 80−140°C.

confirmed that the PLLA sample prepared by cooling at 100°C/min is amorphous, because of the absence of the characteristic band (922 cm^{-1}) of the crystalline phase. In the nonisothermal melt-crystallization, the melted samples were cooled to 0°C at various rates after melted in the same conditions.

The isothermal heat flow curve was integrated to determine the relative crystallinity (X_t) as a function of crystallization time. X_t at any given time was calculated from the integrated area of the DSC curve form $t = 0$ to $t = t$ divided by the integrated area of the whole heat flow curve.

$$X_t = \frac{\int_0^t (dH_c/dt)dt}{\int_0^{t_\infty} (dH_c/dt)dt} \quad (1)$$

where t_∞ denotes the completion time of the crystallization. According to eq. (1), the relationship between X_t and t can be obtained. The crystallization half time ($t_{1/2}$), defined as the time at which $X_t = 0.5$, can be determined from $X_t \sim t$ curve. Besides, $t_{1/2}$ can also be evaluated by the Avrami equation.[40]

RESULTS AND DISCUSSION

WAXD measurement

Figures 1 and 2 present the WAXD patterns of PLLA samples isothermally melt-crystallized and cold-crystallized at different T_cs, respectively. Figures 1 and 2 reveal that at the same T_c, the PLLA samples produced by the melt-crystallization and cold-crystallization show almost the same WAXD patterns, indicating that the crystal structure was insensitive to the initial condition.

It is obvious that the T_c value shows a distinct effect on the WAXD patterns. Notable differences in WAXD patterns are observed between the PLLA samples crystallized at low T_c ($T_c < 110$°C) and high T_c ($T_c \geq 110$°C). The major differences are as follows: (1) Compared with the samples crystallized at $T_c \geq 110$°C, the samples crystallized at $T_c < 110$°C show that the two dominant diffraction peaks, that is, 110/200 and 203 reflections, locate at lower 2θ; (2) In the enlarged Figure 3, it can be seen that at $T_c \geq 110$°C, both the 010 and 015 reflections are more distinct; (3) At $T_c \geq 110$°C, some small diffraction

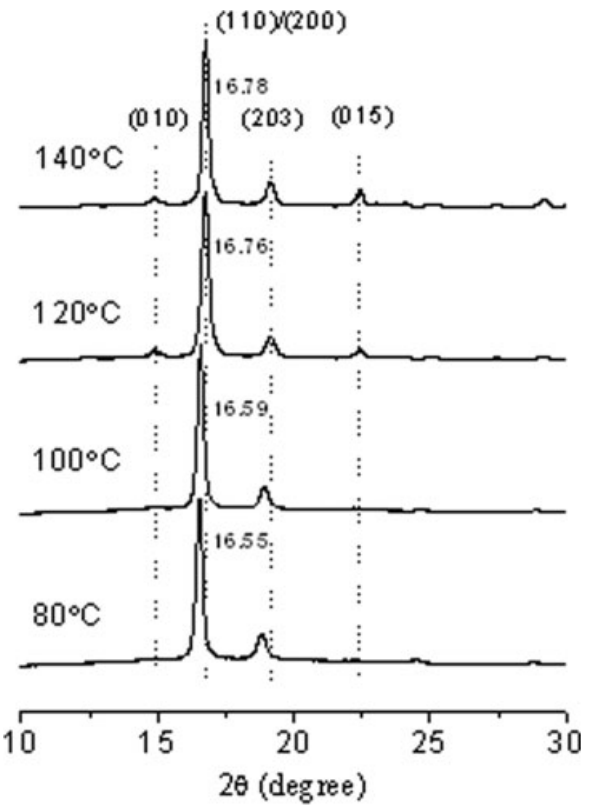

Figure 2 WAXD patterns of PLLA isothermally cold-crystallized at T_c = 80−140°C.

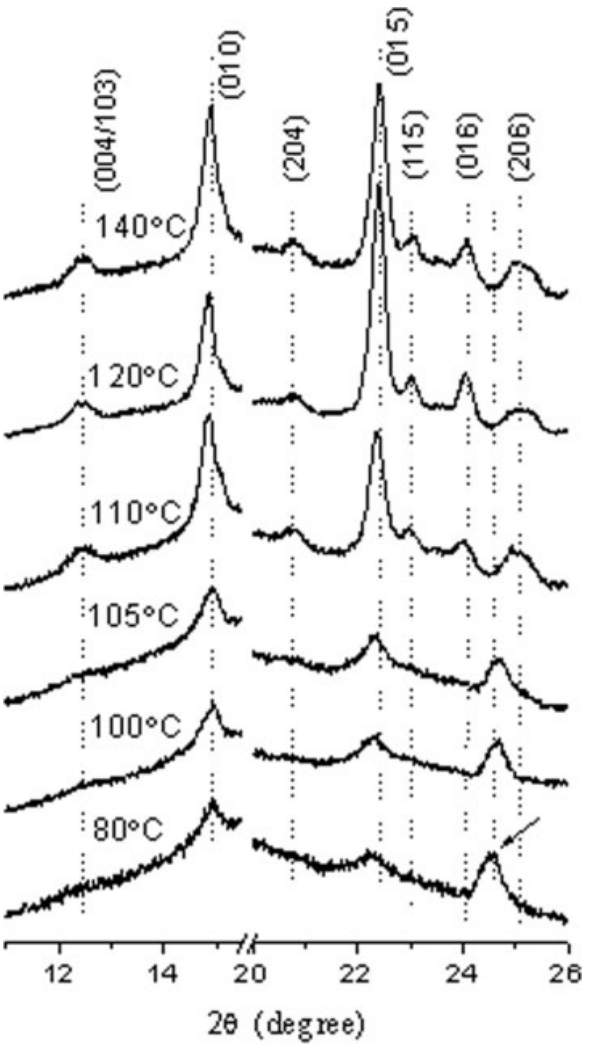

Figure 3 Enlarged WAXD patterns of PLLA melt-crystallized at T_c = 80−140°C.

peaks, locating at 2θ = 12.5°, 20.8°, 23.0°, 24.1°, and 25.1°, which have been assigned to the reflections of 004/103, 204, 115, 016, and 206 planes, respectively,[41] are present, whereas they are absent at T_c < 110°C; (4) The peak situated at 2θ = 24.6° (indicated by the arrow) is characteristic for the samples prepared at T_c < 110°C , and it disappears at $T_c \geq$ 110°C. On the basis of the positions of the reflection peaks of 110/200 and 203 planes, the lattice lengths of these planes are calculated according to the Bragg equation. As shown in Figure 4, with the T_c increases from 100 to 110°C, the lattice lengths of the 110/200 and 203 planes reduce suddenly.

Interestingly, it was found that the temperature 110°C is a critical temperature in the T_c-dependent WAXD patterns. The WAXD patterns of the PLLA samples crystallized at T_c < 110°C distinctly differ from those of the PLLA samples crystallized at $T_c \geq$ 110°C. Moreover, as the T_c value increasing from 80 to 140°C, the WAXD profiles and the lattice lengths of the two main planes, that is, 110/200 and 203, do not change gradually, but change suddenly between 105 and 110°C. Assuming that the same α crystal is also produced at T_c < 110°C, it is difficult to explain the obvious differences between the WAXD patterns and the sudden change of WAXD patterns between 105 and 110°C. So the WAXD results will be analyzed in combination with the FTIR data in the following part.

FTIR spectra

The IR spectra of the amorphous PLLA sample and the semi-crystalline PLLA samples prepared by the isothermal melt-crystallization at different T_cs, especially in the range of 100−120°C, were investigated in detail. To avoid the temperature effect on IR spectral profiles, all these samples were measured at 23°C. Figures 5 and 6 depict the IR spectra and the corresponding second derivatives of the C=O stretching band (1810−1710 cm^{-1}) and 1065−900 cm^{-1} region, respectively. Obviously, the IR spectra of PLLA samples prepared at high and low T_c are different. First, in the ν(C=O) region, besides the dominant band (1759 cm^{-1}), three new bands appearing at 1749, 1768, and 1776 cm^{-1}, respectively, are observed. These three new bands are distinct in the PLLA samples crystallized at high T_c; however, in the PLLA samples crystallized at low T_c these bands are so weak that they can not be clearly observed. As increasing T_c from 105 to 110°C, the 1749 cm^{-1} band suddenly becomes clearer and its intensity increases greatly. Also, the 1776 cm^{-1} band shows the similar tendency. On the other hand, from the second derivatives of the 1759 cm^{-1} band, it is

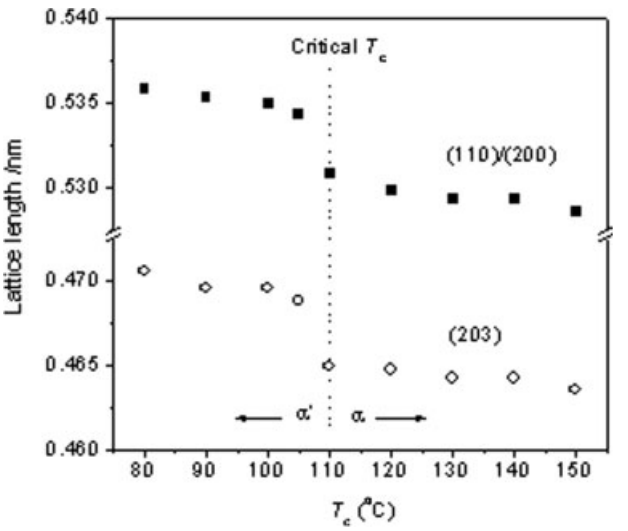

Figure 4 Temperature dependent *d*-spacings of the 110/200 and 203 lattice planes as calculated from 2θ positions shown in Figure 1 by Bragg equation.

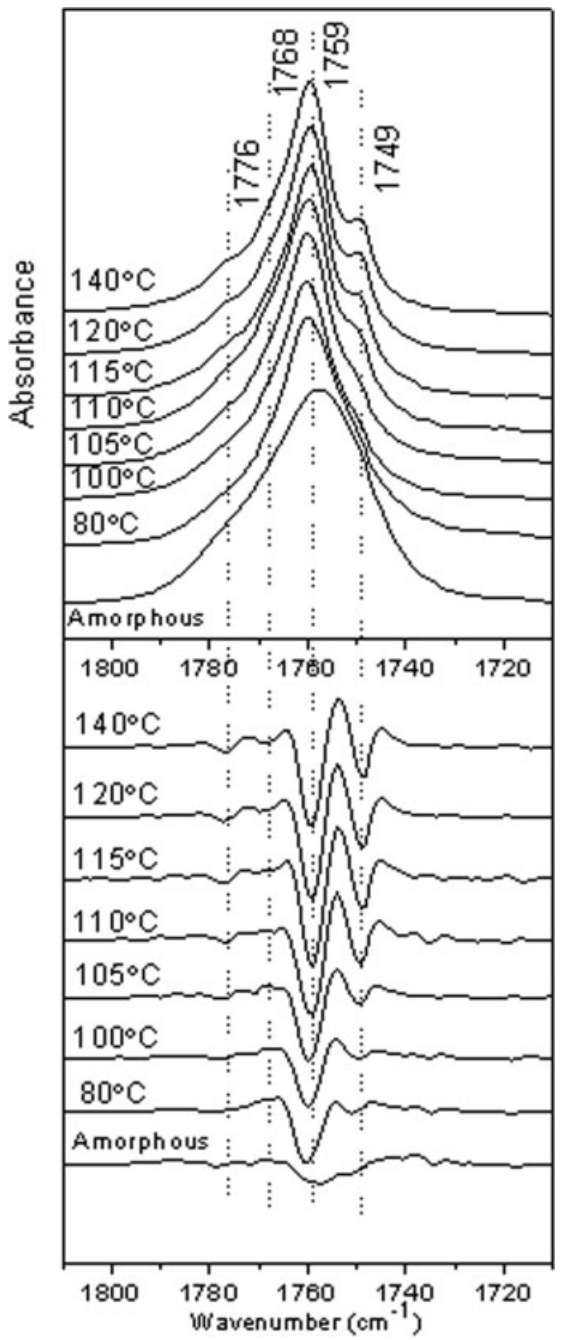

Figure 5 IR spectra (upper) and their second derivative (lower) in the 1810−1710 cm^{-1} region of amorphous PLLA and crystalline PLLA isothermally melt-crystallized at T_c = 80−140°C.

seen that this dominant band almost fixes at 1759 cm^{-1} at $T_c \geq 110$°C. Nevertheless, at $T_c < 110$°C, it shifts toward higher wave number by about 1 cm^{-1}.

Second, it is also found from Figure 6 that the temperature of 110°C is also a critical T_c for the 922 cm^{-1} band, which is considered to be very sensitive to helical chain conformation of the PLLA crystal.[42] At $T_c \geq 110$°C, this band almost fixes at 922 cm^{-1}, whereas at $T_c < 110$°C, it shifts about 2 cm^{-1} toward higher wave number. Third, interestingly, in the 1045 cm^{-1} band, which has been assigned to the stretching vibration of the C—CH_3 group, as for the PLLA samples crystallized at $T_c \geq 110$°C a small band situated at about 1053 cm^{-1} is present, whereas this band is absent for the PLLA samples crystallized at $T_c < 110$°C.

Generally, the crystallization is accompanied by the development of specific interactions, including

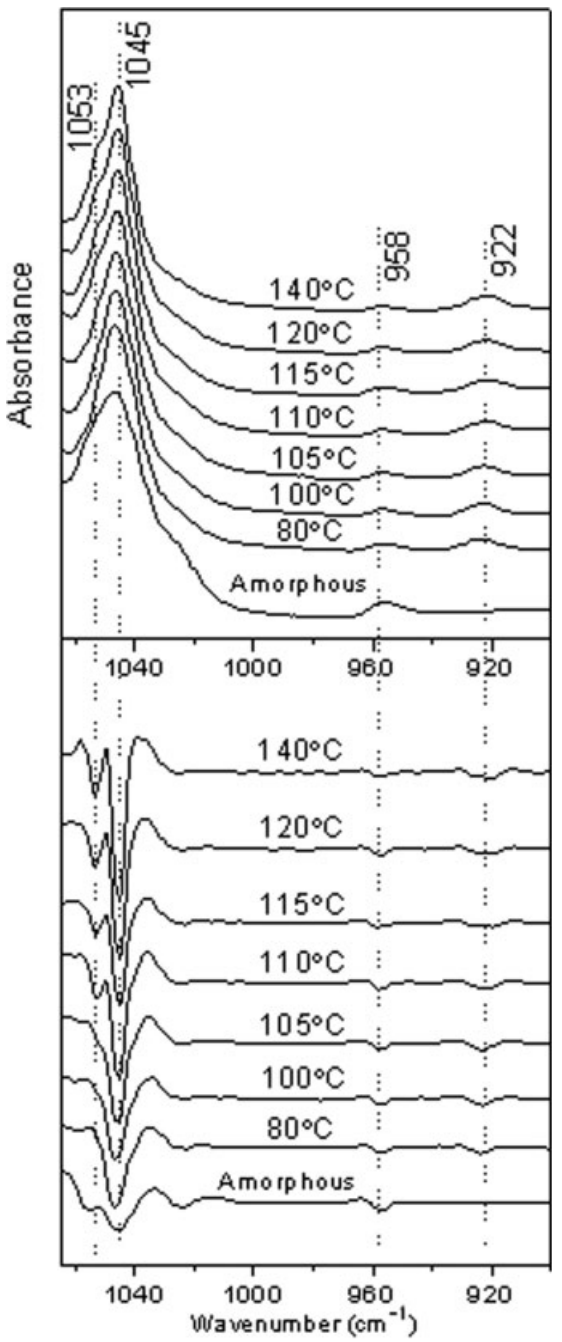

Figure 6 IR spectra (upper) and their second derivative (lower) in the 1065−900 cm^{-1} region of amorphous PLLA and crystalline PLLA isothermally melt-crystallized at T_c = 80−140°C.

both intramolecular and intermolecular interactions.[43] These interactions are suspected to account for some of multiplicity of peaks recorded in vibrational spectra of a number of crystalline polymers, including polyethylene, polyoxymethylene, and polyethylene.[44] This interesting spectroscopic phenomenon has been termed correlation field splitting (or Davydov splitting or factor group splitting).[43] As aforementioned, the band-splitting phenomenon resulted by the correlation field is also present in the IR spectra of the crystallized samples of PLLA, such as the 1749, 1768, and 1776 cm^{-1} bands in the carbonyl stretching region and the 1053 cm^{-1} band in the C—CH_3 stretching region. The band-splitting of carbonyl stretching band has been assigned to the interaction between the C=O groups of the adjacent polymer chains.[42] Similar to the results in the reference,[27] the band-splitting of the CH_3 symmetric deformation mode around 1387 cm^{-1} and the CH_3 asymmetric deformation mode around 1457 cm^{-1}, which is ascribed to the dipole–dipole interaction because of the interchain packing of CH_3 groups in the crystal unit cell of PLLA, was also observed in our study.

Since the C—CH_3 groups are separated alternately by the C=O groups along the polymer chain of PLLA, it is considered that the distance between the neighboring C—CH_3 groups is similar with that of the C=O groups, which is estimated to be 0.326 nm[7] and is larger than the distance (~ 0.270 nm) for inducing the intrachain dipole–dipole interaction.[43] Accordingly, it seems very likely that the splitting of ν(C—CH_3) around 1053 cm^{-1} is also not caused by the intrachain interaction but caused by the interchain interaction between the adjacent C—CH_3 groups in the unit cell of PLLA crystal.

It should be noted that, corresponding to the previous WAXD data, 110°C is also a critical T_c for the IR spectra of the PLLA samples crystallized at different T_cs. As aforementioned, the differences among the IR spectra of PLLA samples crystallized at $T_c < 110$°C and $T_c \geq 110$°C are chiefly observed as: (1) the band shifting of ν(C=O) and the 922 cm^{-1} band; (2) the band-splitting of ν(C=O), ν(CH_3), ν(C—CH_3) and δ(CH_3). Surprisingly, these differences of IR spectra are almost entirely associated with the vibration mode of the C=O, CH_3 and C—CH_3 side groups, such as, ν(C=O), ν(CH_3), ν(C—CH_3), δ(CH_3), and γ(CH_3).

POM analysis

Generally, the difficulty in nucleation at low undercooling and the poor diffusivity at high undercooling endure the crystallization behavior of macromolecules with a bell-shaped growth dependence on the crystallization temperature. Nevertheless, in the case of PLLA, its crystalline growth behavior is very unusual. The T_c dependence of the spherulite radius growth rates (G) is shown for PLLA in Figure 7. The G value shows a bimodal T_c dependence, with a minimum located at nearby 110°C between two peaks. Usually, in the crystallization process of polymer, because of the different growth kinetics, the presence of more than one crystallographic form usually causes the multi-peaked spherulite growth kinetics.[45]

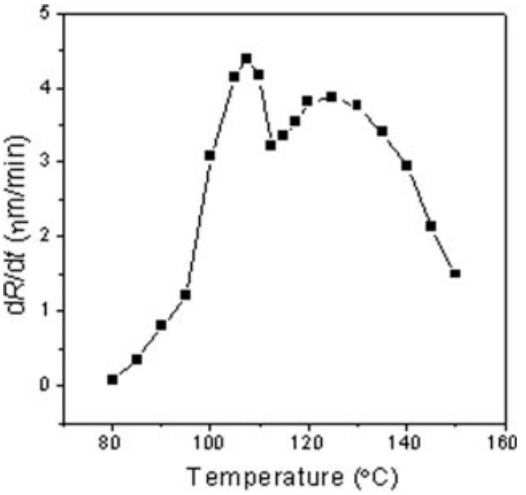

Figure 7 Spherulites radius growth rate of PLLA measured in isothermal melt-crystallization at T_c = 80−140°C.

Figure 8 shows the spherulite morphology of the PLLA sample crystallized at 100 and 140°C. All the spherulites have a negative birefringence, with the *a*-axis of the orthorhombic unit cell being oriented in the radial direction[46]. Almost no difference on the spherulite morphologies is observed between the PLLA samples crystallized at low and high T_c. Besides, almost no change is observed in the spherulite morphologies during the isothermal crystallization at a certain T_c.

DSC measurement

Crystallization behavior of PLLA was also surveyed by DSC under the nonisothermal conditions with various cooling rates and the isothermal conditions at different T_cs, respectively. Nonisothermal crystallization DSC curves with the different cooling rates are depicted in Figure 9. The crystallization of PLLA is very slow, and it can not crystallize completely when the cooling rate is larger than 5°C/min. In the cooling scanning at 2.5°C/min, a small shoulder located at 110−130°C was detected before an appearance of dominant crystallization peak. The differential of heat flow to temperature $[\Delta(\Delta H/\Delta t)/\Delta T]$ is smaller at T_c = 110−130°C, but it increases suddenly at about 110°C. This indicates that the change of the

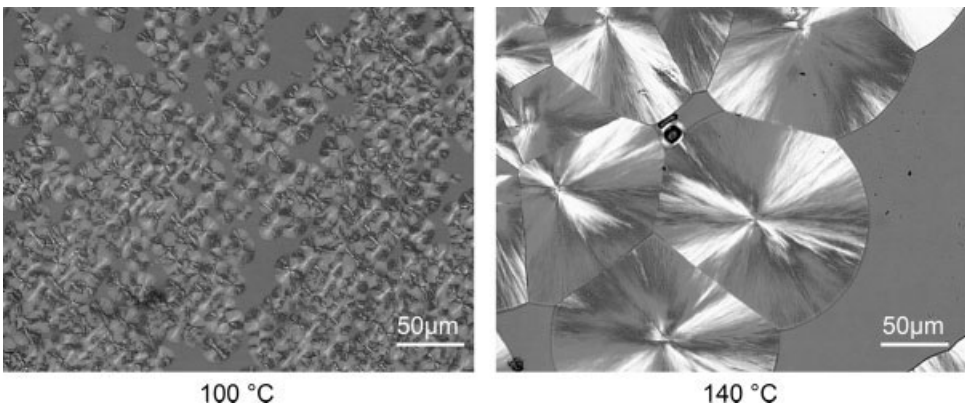

Figure 8 Optical micrographs of PLLA isothermally melt-crystallized at 100 and 140°C.

crystallization mechanism maybe take place in this region. The half time ($t_{1/2}$) derived from the DSC results in isothermal melt-crystallization at various T_cs is displayed in Figure 10. It was found that, very similar with the POM results, this curve is discontinuous between 100 and 120 °C. An inflexion is observed at around 110°C, and the curve is divided into two parts by this inflexion.

Polymorphic crystallization of PLLA

The results show that the WAXD and IR data are consistent very well with each other. The characteristic of the WAXD patterns and IR spectra of the PLLA samples crystallized at high T_c are the same with those of the PLLA α crystal,[14] leading us to conclude that only the α crystal was produced at high T_c. Interestingly, 110°C is found to be a critical T_c for both the WAXD patterns and IR spectra. Furthermore, it has been also reported that, with increasing T_c, the heats of fusion of the isothermally crystallized PLLA samples at different T_cs increase suddenly between 100 and 125°C.[26] Therefore, it is concluded that at low and high T_c the different crystal forms are produced.

Because of the absence of the IR characteristic band of PLLA β crystal, 912 cm^{-1} band, and the characteristic diffraction peak of the 003 plane of the PLLA β form, located at around $2\theta = 30.0°$,[12,13] it is concluded that the produced crystal at low T_c is not the β crystal. Combining these results and the peculiar crystallization behavior of PLLA, it should be reasonable to propose that at low T_c, another crystal modification, which has been named as α′ form, is produced. What is more, 110°C is critical T_c to produce the α′ and α crystals, and at $T_c < 110$°C and $T_c \geq 110$°C, the α′ and α crystals are mainly developed, respectively.

Crystalline structure of PLLA α′ crystal

Because of the presence of the 922 cm^{-1} band in the IR spectra of the α′ crystal, and the very similar

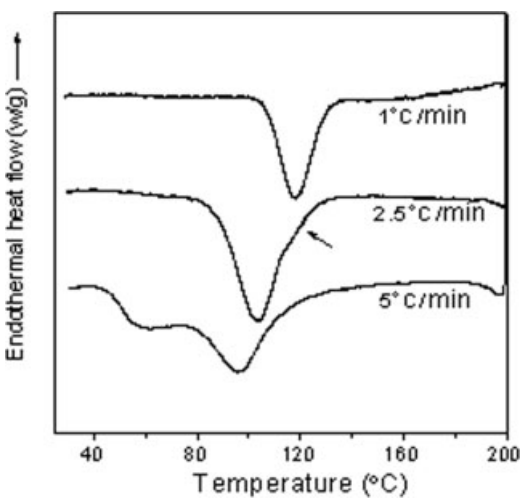

Figure 9 Nonisothermal melt-crystallization DSC curves of PLLA at different cooling rate. (The arrow indicates the shoulder appeared before the dominant peak).

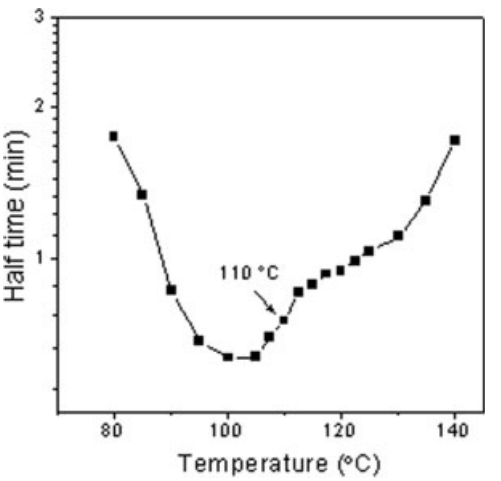

Figure 10 The half time of PLLA isothermally melt-crystallizated at different T_cs.

WAXD patterns between the α′ and α crystals, it has been proposed that like the α crystal, the polymer chains of the α′ crystal also have the 10_3 conformation and pack into the orthorhombic or pseudo-orthorhombic unit cell.[27] On the basis of the WAXD results of PLLA samples crystallized at T_c = 80°C and 150°C, the *d*-spacings of the various reflection planes of the α′ and α crystals of PLLA were calculated and summarized in Table I. According to the *d*-spacings of the 200 and 010 planes, the cell parameters of the α′ (a = 1.072 nm, b = 0.594 nm) and α (a = 1.058 nm, b = 0.595 nm) crystals were evaluated. In addition, because the *d*-spacings of the 010 and 015 planes of the α′ and α are very similar, it is considered that the cell parameter c of the α′ and α is similar. It reveals that the a value of the α′ crystal is a little larger than that of the α crystal, indicating that in the α′ crystal the distance between the two antiparallel helical chains within the unit cell is larger. For this reason, the interchain interactions between the side groups in the α′ crystal are weaker than those of the α crystal, and it will lead the differences of IR spectra between the α′ and α crystals and less band-splitting phenomenon in the spectra of the α′ crystal.

However, the difference between the cell dimension of the α′ and α crystals is very small, so that it is possibly not enough to cause experimentally observed considerable dissimilarities between the IR spectra of the PLLA α′ and α crystals. Thus, it is suspected that there are other differences between the structures of the PLLA α′ and α crystals. From the IR band assignments of the α′ and α crystals tabulated in Table II, it can seen that the large differences between the IR spectra of the α′ and α crystals are chiefly related to the vibration modes induced by the interchain interaction of the side groups, including C=O, CH_3, and C—CH_3. Usually, it is believed that the structural changes of various functionalities within a polymer chain occur cooperatively during the crystallization, and finally this structural adjustment will lead to the functionalities of the polymer chain to reach toward the more stable state. At higher T_c, the viscosity of crystallization system is smaller, inducing that the structural adjustment and diffusion of polymer chains are easier. Accordingly, at higher T_c it is easier for the various functionalities, especially the side groups, to reach the ideal stable state with the lowest packing energy. Thus, structural adjustment maybe induces the different arrangement and packing of the side groups in the unit cell between the PLLA α′ and α crystals which are produced at low and high T_c, respectively.

From the potential energy calculation, it has been confirmed that the side groups in the polymer chains of the α crystal almost pack in the ideal state with the minimum packing energy.[9] Therefore, compared with the PLLA α′ crystal, the side groups, including C=O, CH_3, and C—CH_3, in the unit cell of the α crystal are more ordered and denser, which leads to the dissimilarities of the cell dimension and interchain interactions between the α′ and α crystals. The molecular interactions between the neighboring chains of the α crystal are stronger, leading to the more distinct and intensive splitting of IR banding. Moreover, owing to the more ordered and denser packing of the side groups, more WAXD reflection peaks are observed for the PLLA α crystal.

TABLE I
X-ray *d*-Spacings of the α′ and α Crystals of PLLA

Observed *d*-spacings (nm)		
α′	α	Lattice plane (*hkl*)
Not observed	0.711	004/103
0.594	0.595	010
0.536	0.529	110/200
0.471	0.463	203
Not observed	0.428	204
0.399	0.397	015
Not observed	0.386	115
Not observed	0.370	016
0.363	Not observed	Unclear
Not observed	0.355	206

TABLE II
Differences Between FTIR Vibration Modes of the α′ and α Crystals of PLLA

IR frequencies (cm^{-1})		
α′	α	Assignment
2997	2997	$\nu_{as}(CH_3)$
	3006	
2945	2945	$\nu_s(CH_3)$
	2964	
1760	1759	ν(C=O)
	1749	
	1768	
	1776	
1457	1457	$\delta_{as}(CH_3)$
	1443	
1387	1387	$\delta_s(CH_3)$
	1381	
	1396	
1045	1045	ν(C—CH_3)
	1053	
924	922	r(CH_3) + ν(C—C)

CONCLUSION

According to the present study on the effect of T_c on the crystallization behavior of PLLA by using WAXD and IR, the following points are clarified. 110°C is a critical T_c for the crystalline structure and crystallization kinetics of PLLA. At T_c < 110°C and $T_c \geq$ 110°C, the α′ and α crystals were mainly pro-

duced, respectively. The cell parameters of α′ crystal were elucidated: $a = 1.072$ nm, $b = 0.594$ nm, which is a little larger than those of the α crystal, due to the more ordered and denser packing of polymer chains in the α crystal. The discontinuous crystallization kinetics, that is, double peaks of the $G \sim T_c$ curve and the two parts of the $T_c \sim t_{1/2}$ profile in low and high T_c are due to the growth of the α′ and α crystals, respectively. Because of the different structures of PLLA α′ and α crystals, it is considered that the mechanical, thermal properties, and the biodegradability of PLLA crystallized at various T_c are probably different. Therefore, the properties of PLLA can be optimized by changing the crystallization process, and our future work will focus on the difference of properties between PLLA α′ and α crystals.

The authors gratefully thank Dr. Kazue Ueda and Unitika Co. LTD. (Kyoto, Japan) for kindly supplying the PLLA sample.

References

1. Södergård, A.; Stolt, M. Prog Polym Sci 2002, 27, 1123.
2. Jain, R. A. Biomaterials 2000, 21, 2475.
3. Ikada, Y.; Tsuji, H. Macromol Rapid Commun 2000, 21, 117.
4. Sinclair, R. G. Pure Appl Chem A 1996, 33, 585.
5. Aou, K.; Hsu, S. L. Macromolecules 2006, 39, 3337.
6. De Santis, P.; Kovacs, J. Biopolymers 1968, 6, 299.
7. Hoogsteen, W.; Postema, A. R.; Pennings, A. J.; Ten, B. G.; Zugenmaier, P. Macromolecules 1990, 23, 634.
8. Kobayshi, J.; Asahi, T.; Ichiki, M.; Okikawa, A.; Suzuki, H.; Watanabe, T.; Fukada, E.; Shikinami, Y. J Appl Phys 1995, 77, 2957.
9. Sasaki, S.; Asakura, T. Macromolecules 2003, 36, 8385.
10. Eling, B.; Gogolewski, S.; Pennings, A. J. Polymer 1982, 23, 1587.
11. Puiggali, J.; Ikada, Y.; Tsuji, H.; Cartier, L.; Okihara, T.; Lotz, B. Polymer 2000, 41, 8921.
12. Sawai, D.; Takahashi, K.; Imamura, T.; Nakamura, K.; Kanamoto, T.; Hyon, S. H. J Polym Sci Part B: Polym Phys 2002, 40, 95.
13. Sawai, D.; Takahashi, K.; Sasashige, A.; Kanamoto, T.; Hyon, S. H. Macromolecules 2003, 36, 3601.
14. Brizzolara, D.; Cantow, H. J.; Diederichs, K.; Keller, E.; Domb, A. J. Macromolecules 1996, 29, 191.
15. Cartier, L.; Okihara, T.; Ikada, Y.; Tsuji, H.; Puiggali, J.; Lotz, B. Polymer 2000, 41, 8909.
16. Iannace, S.; Nicolais, L. J Appl Polym Sci 1997, 64, 911.
17. Miyata, T.; Masuko, T. Polymer 1998, 39, 5515.
18. Abe, H.; Kikkawa, Y.; Inoue, Y.; Doi, Y. Biomacromolecules 2001, 2, 1007.
19. Di Lorenzo, M. L. Polymer 2001, 42, 9441.
20. Ohtani, Y.; Okumura, K.; Kawaguchi, A. J Macromol Sci Part B: Phys 2003, 3/4, 875.
21. Pluta, M.; Galeski, A. J Appl Polym Sci 2002, 86, 1386.
22. Yasuniwa, M.; Tsubakihara, S.; Sugimoto, Y.; Nakafuku, C. J Polym Sci Part B: Polym Phys 2004, 42, 25.
23. Krikorian, V.; Pochan, D. J. Macromolecules 2005, 38, 6520.
24. Wang, Y.; Mano, J. F. Eur Polym J 2005, 41, 2335.
25. Di Lorenzo, M. L. Eur Polym J 2005, 41, 569.
26. Cho, T. Y.; Strobl, G. Polymer 2006, 47, 1036.
27. Zhang, J. M.; Duan, Y.; Sato, H.; Tsuji, H.; Noda, I.; Yan, S.; Ozaki, Y. Macromolecules 2005, 38, 8012.
28. Yasuniwa, M.; Tsubakihara, S.; Iura, K.; Ono, Y.; Dan, Y.; Takahashi, K. Polymer 2006, 47, 7554.
29. Perego, G.; Cella, G. D.; Bastioli, C. J Appl Polym Sci 1996, 59, 37.
30. Lee, J. K.; Lee, K. H.; Jin, B. S. Eur Polym J 2001, 37, 907.
31. Ho, R. M.; Lin, C. P.; Tsai, H. Y.; Woo, E. M. Macromolecules 2000, 33, 6517.
32. De Rosa, C.; Gargiulo, M. C.; Auriemma, F.; Ruiz de Ballesteros, O.; Razavi, A. Macromolecules 2002, 35, 9083.
33. Rueda, D. R.; García Gutiérrez, M. C.; Ania, F.; Zolotukhin, M. G.; Baltá Calleja, F. J. Macromolecules 1998, 31, 8201.
34. Ho, R. M.; Cheng, S. Z. D.; Hsiao, B. S.; Gardner, K. H. Macromolecules 1994, 27, 2136.
35. Alamo, R. G.; Kim, M. H.; Galante, M. J.; Isasi, J. R.; Mandelkern, L. Macromolecules 1999, 32, 4050.
36. Medellin-Rodriguez, F. J.; Larios-Lopez, L.; Zapata-Espinoza, A.; Davalos-Montoya, O.; Phillips, P. J.; Lin, J. S. Macromolecules 2004, 37, 1799.
37. Meille, S. V.; Romita, V.; Caronna, T.; Lovinger, A. J.; Catellani, M.; Belobrzeckaja, L. Macromolecules 1997, 30, 7898.
38. Lotz, B.; Graff, S.; Wittman, J. C. J Polym Sci: Polym Phys Ed 1986, 24, 2017.
39. Nishimura, Y.; Takasu, A.; Inai, Y.; Hirabayashi, T. J Appl Polym Sci 2005, 97, 2118.
40. Pan, P.; Zhu, B.; Kai, W.; Serizawa, S.; Iji, M.; Inoue, Y. J Appl Polym Sci 2007, 105, 1511.
41. Miyata, T.; Masuko, T. Polymer 1997, 38, 4003.
42. Kister, G.; Cassanas, G.; Vert, M. Polymer 1998, 39, 267.
43. Lagaron, J. M. Macromol Symp 2002, 184, 19.
44. Lagaron, J. M.; Powell, A. K.; Davidson, N. S. Macromolecules 2000, 33, 1030.
45. Gan, Z. H.; Kuwabara, K.; Abe, H.; Iwata, T.; Doi, Y. Biomacromolecules 2004, 5, 371.
46. Kalb, B.; Pennings, A. J. Polymer 1980, 21, 607.